Hindawi
Mathematical Problems in Engineering
Volume 2018, Article ID 7072032, 15 pages
https://doi.org/10.1155/2018/7072032

Research Article

Output Information Based Fault-Tolerant Iterative Learning Control for Dual-Rate Sampling Process with Disturbances and Output Delay

Hongfeng Tao , Yan Liu, and Huizhong Yang

Key Laboratory of Advanced Process Control for Light Industry of Ministry of Education, Jiangnan University, Wuxi 214122, China

Correspondence should be addressed to Hongfeng Tao; taohongfeng@hotmail.com

Received 18 August 2017; Accepted 8 February 2018; Published 19 March 2018

Academic Editor: Andrzej Swierniak

For a class of single-input single-output (SISO) dual-rate sampling processes with disturbances and output delay, this paper presents a robust fault-tolerant iterative learning control algorithm based on output information. Firstly, the dual-rate sampling process with output delay is transformed into discrete system in state-space model form with slow sampling rate without time delay by using lifting technology; then output information based fault-tolerant iterative learning control scheme is designed and the control process is turned into an equivalent two-dimensional (2D) repetitive process. Moreover, based on the repetitive process stability theory, the sufficient conditions for the stability of system and the design method of robust controller are given in terms of linear matrix inequalities (LMIs) technique. Finally, the flow control simulations of two flow tanks in series demonstrate the feasibility and effectiveness of the proposed method.

1. Introduction

In industrial applications, many engineering plants operate in continuous time while the system inputs and outputs are sampled, yielding discrete-time signals. Moreover, due to the hardware limitations, process characteristics, and other reasons, sampling each variable with the same frequency is not necessary and realistic. Therefore, the measurable output and input information is usually sampled in different rates from different types of sensors, manual sampling, or laboratory analyses [1, 2]. These systems are often termed as multirate sampling process and dual-rate sampling process is a special case; sometimes the sampling periods of the slow rate sampled variables are integer multiples of the fast rate sampled ones [3]. For example, the control of the bottom and top composition products of a distillation column by acting on the reflux and vapor flow rates is a typical case, where the input control signals can be rapidly adjusted, while the infrequent and delayed composition measurements are only obtained by gas chromatography [4]. In some vehicle control systems, displacement and velocity are measured by using ultrasonic sensors; the two different groups of sensors are located at different locations of the vehicle and have different sampling periods [5]. During the last several decades, this corresponding control problem has attracted considerable attention, including the model identification [6–8] and control algorithms [9–11]. But the control problem of dual-rate sampling systems still has achieved relatively little research results compared with the single-rate sampling case. Moreover, to the best of our knowledge, there are few papers dealing with iterative learning control (ILC) problems for dual-rate sampling process with time delay and actuator fault.

The idea of ILC arose from Uchiyama in 1978 [12]; it represents a powerful approach for high performance tracking control of systems, which execute the same task over a finite duration repeatedly with a given desired trajectory and reset to the starting location once each execution is complete. Each execution of the task is known as a trial, or pass, and its duration is termed the trial length. ILC is currently mainly used to control single-rate sampling process. Compared with standard control scheme, the distinguishing feature of the ILC dynamic sequence of operations is to use the information from previous trials to update the control signal applied on the next one; the major advantage of ILC is the ability to improve system performance from trial to trial and include temporal information from previous trials that would be noncausal in standard systems. Over the past few decades, ILC has drawn significant research attention and increasingly been employed in many industrial processes, such as traffic system [13], networked stochastic system [14], robotic manipulator system [15], multiagent system [16], chemical pharmaceutical crystallization [17], and industrial injection molding batch processes [18].

The design of an ILC law starts, as always, with performance specifications where the novel feature for ILC is the reference trajectory or vector, which is assumed to be the same for all trials in most of the ILC literature. In the case of discrete dynamics, let $y(t,k)$, $u(t,k)$ denote the output and input, respectively, on trial k; t denotes the sampling number over the trial duration. Then if the error on trial k is $e(t,k) = y_r(t) - y(t,k)$, where $y_r(t)$ denotes the reference signal, and the basic ILC design problem is to construct a sequence of input function that forces the error sequence $\{e_k\}_{k\geq 0}$ and input sequence $\{u_k\}_{k\geq 0}$ to converge to zero and u_∞, respectively, or to within an acceptable tolerance, u_∞ is termed learned control. It is a common approach to ILC design for discrete dynamics to use the lifting technique [19]. For the SISO systems with a nature extension to the multiple-input multiple-output (MIMO) systems, the input and output on any trial can be represented by supervectors formed by assembling the values at the sample instants into a column vector. Once the ILC law is applied, the propagation of the error can be represented by a linear difference equation and discrete linear systems theory can be utilized for trial-to-trial error convergence analysis and control law design.

Given the finite trial length, trial-to-trial error convergence can occur even if the system is unstable since such a system can only produce a bounded output over a finite time duration. Literature reviews [20–22] confirm that an alternative approach to ILC design is to first apply a feedback control law to produce acceptable dynamics along the trial and then apply ILC to accomplish trial-to-trial error convergence of the resulting 2D system. A drawback of the two-step synthesis procedure is that it does not lead to an optimal combination of the feedback and feedforward actions. Based on an abstract model in a Banach space setting, repetitive process is a particular subclass of 2D system that operates over a subset of the upper right quadrant of the 2D plane and is characterized by a series of sweeps, or passes, through a set of dynamics defined over a finite duration known as the pass length. It is a nature setting for ILC analysis and design; the main advantage is that it gives a systematic way to simultaneously consider behaviour along the time axis and from trial to trial [23]. A detailed treatment of the dynamics of these processes, including their origins in the modeling of mining operations, can be found in [24].

Time delay is also frequently encountered in the transmission of material or information between different parts of a system, including biology, chemistry, economics, population dynamics, and engineering applications. Time delay is one of the main causes of instability and poor performance in process control systems [25, 26], and currently many ILC algorithms have been applied to time delay single-rate sampling process by treating them as batch processes in a finite time on every trial. For example, a robust 2D closed-loop ILC combined with the output feedback scheme has been applied to batch processes with state delay and time-varying uncertainties [27, 28]. Composite iterative learning feedback controllers combined with state and output information are designed in [29]; then the sufficient conditions for delay dependent stability are obtained. However, these proposed methods are just based on the single-rate sampling process model, so that they cannot be directly applied to dual-rate sampling processes. Furthermore, these methods only use consistent slow sampling data and do not fully utilize all sampling data with different sampling intervals to improve control performance.

Moreover, the involved industrial control systems under challenging environment are vulnerable to faults. A fault in a single component may have major efforts on the large system as a whole. Actuator faults will reduce the stability and performance of control systems and may even cause complete breakdown of these systems. Fault-tolerant control is a special action that ensures a fail-safe operation under real-time conditions if components in the control system fail or become faulty [30]. Fault-tolerant ILC design which is sensitive to faults is especially required in application for ILC scheme due to the repeated nature of the control actuator. The extensions to deal with faults for ILC systems receive increasing attentions [31, 32]. For example, a robust fault-tolerant iterative learning control design method is proposed and illustrated by an electric motor system in [31] and also [32] gives iterative learning fault-tolerant control for a class of linear differential time delay uncertain systems with actuator faults in finite frequency domains. The challenge of fault-tolerant control here is how to design a reliable ILC scheme against fault based on the inconsistent dual-rate sampling input and output information with time delay.

This paper develops new results for ILC design applied to time delay dual-rate sampling process with the following contributions:

(i) The output information based ILC law design is extended to the fault-tolerant control problem for dual-rate sampling process with time delay and actuator faults.

(ii) Monotonic trial-to-trial error convergence conditions for the controlled ILC dynamics are derived.

(iii) Robust control issue for disturbance attenuation performance is solved.

This paper is organized as follows: Section 2 describes a dual-rate sampling process with output delay and disturbance in the ILC setting by the state-space model with actuator faults; then it is transformed into a discrete system model form in slow sampling rate without time delay by using the lifting technology. Section 3 formulates the output information based fault-tolerant ILC design problem in the repetitive process setting. Some repetitive process stability theories are given as background in Section 4. Then the sufficient conditions for the stability of the controlled dynamic and the design method of robust controller are analyzed and given in corresponding linear matrix inequalities form in Section 5. Section 6 verifies the effectiveness of the proposed method by the flow control simulations of two flow tanks in series. Finally, some conclusions are given in Section 7.

Throughout this paper, the null and identity matrices with the required dimensions are denoted by 0 and I, respectively, and the notation $X \prec Y$ (resp., $X \succ Y$) is used to represent the negative definite (resp., positive definite) matrix $X - Y$. The notation $(\star)$ denotes the transpose of elements in the symmetric position in a matrix. The symbol $\text{diag}\{X_1, X_2, \ldots, X_n\}$ denotes a block-diagonal matrix with diagonal blocks $X_1, X_2, \ldots, X_n$ and $\text{sym}(\Lambda) = \Lambda + \Lambda^T$. The symbol $\lfloor x \rfloor$ represents the largest integer which is less than or equal to x.

2. System Description

Consider a class of SISO linear continuous processes P_c in Figure 1 with output delay and disturbance; system dynamics are described in the ILC setting by the following state-space model:

$$\begin{aligned} \dot{x}(t,k) &= A_c x(t,k) + B_c u(t,k) + D_c w(t,k), \\ y(t,k) &= C_c x(t-\tau,k), \quad 0 < t < \alpha, \end{aligned} \tag{1}$$

where the symbol $k \geq 0$ denotes the trial number, α is the fixed and finite trial length, $x(t,k) \in \mathbb{R}^n$, $u(t,k) \in \mathbb{R}^1$, $y(t,k) \in \mathbb{R}^1$, and $w(t,k) \in \mathbb{R}^m$ are the system state, input, output, and disturbance vectors, respectively, τ is the time delay constant, and A_c, B_c, C_c, and D_c are system matrices of appropriate dimensions. Without loss of generality, assume $x(t,k) = x_{0,k}$, $t \in [-\tau, 0]$, on each trial.

To include actuator faults, let $u^F(t,k)$ represent the failed actuator with the following fault model [32]:

$$u^F(t,k) = \Gamma u(t,k), \tag{2}$$

where the actuator failure parameter Γ is unknown, but it satisfies the following condition:

$$0 \leq \underline{\Gamma} \leq \Gamma \leq \overline{\Gamma}. \tag{3}$$

The parameters $\underline{\Gamma}$ ($\underline{\Gamma} \leq 1$), $\overline{\Gamma}$ ($\overline{\Gamma} \geq 1$) in this fault model, are assumed to be known. When $\Gamma = 1$, it corresponds to the normal case $u^F(t,k) = u(t,k)$; when $\Gamma = 0$, it covers the outage case; $0 < \underline{\Gamma} \leq \Gamma < 1$ and $1 < \Gamma \leq \overline{\Gamma}$ correspond to partial failures, for example, partial degradation of an actuator or the abnormal case when the faulty actuator output is larger than the normal controller output. Introduce

$$\begin{aligned} q &= \frac{\left(\overline{\Gamma} + \underline{\Gamma}\right)}{2}, \\ q_0 &= \frac{\overline{\Gamma} - \underline{\Gamma}}{\overline{\Gamma} + \underline{\Gamma}}, \end{aligned} \tag{4}$$

and define $\Gamma_0 = (\Gamma - q)/q$; then by using (4), the unknown failure parameter Γ can be written as

$$\Gamma = \left(I + \Gamma_0\right) q, \tag{5}$$

where

$$\left|\Gamma_0\right| \leq q_0 \leq 1. \tag{6}$$

Therefore, the continuous process P_c of (1) with actuator fault can be described by

$$\begin{aligned} \dot{x}(t,k) &= A_c x(t,k) + B_c \Gamma u(t,k) + D_c w(t,k), \\ y(t,k) &= C_c x(t-\tau,k), \quad 0 < t < \alpha. \end{aligned} \tag{7}$$

For process (7), the discrete-time signal $u(nT_1,k)$ with sampling period $T_1 = ph$ is maintained as a continuous-time input signal $u(t,k)$ using a zero-order hold H_{T_1} in Figure 1; then

$$u(t,k) = u\left(nT_1,k\right), \quad nT_1 < t < (n+1)\,T_1; \tag{8}$$

the continuous-time output signal $y(t,k)$ is sampled by a sampler S_{T_2} with sampling period $T_2 = qh$ to get discrete-time output signal $y(nT_2,k)$, where $h > 0$ is the basic sampling period and p and q are the two positive coprime integers. For such a dual-rate sampling process, the measurable input-output data is $\{u(nT_1,k), y(nT_2,k),\ n = 0,1,2,\ldots\}$; $\{u(nT_1 + ih,k), y(nT_2 + jh,k), i = 1,2,\ldots,p-1,\ j = 1,2,\ldots,q-1\}$ are unknown [33]. Moreover, in order to obtain the system model of dual-rate sampling process, the continuous process P_c is first discretized with sampling period h to obtain the discrete system model P_h:

$$\begin{aligned} x(nh+h,k) &= A_h x(nh,k) + B_h \Gamma u(nh,k) \\ &\quad + D_h w(nh,k), \\ y(nh,k) &= C_h x(nh - dh,k), \end{aligned} \tag{9}$$

where $A_h = e^{A_c h}$, $B_h = \int_0^h e^{A_c t} dt B_c$, $C_h = C_c$, and $D_h = \int_0^h e^{A_c t} dt D_c$, $d = \lfloor \tau/h \rfloor$.

For process P_h, let $T \coloneqq pqh$ be the frame period to denote the cycle sampling period of the system, then using symbol npq instead of n in (9), we have

$$\begin{aligned} x(nT,k) &= x(npqh,k) = A_h x((npq-1)h,k) \\ &\quad + B_h \Gamma u((npq-1)h,k) + D_h w((npq-1)h,k) \\ &\quad = A_h \{A_h x((npq-2)h,k) \\ &\quad + B_h \Gamma u((npq-2)h,k) + D_h w((npq-2)h,k)\} \\ &\quad + A_h x((npq-1)h,k) + B_h \Gamma u((npq-1)h,k) \\ &\quad + D_h w((npq-1)h,k) = \cdots = A_h^d x(nT - dh,k) \\ &\quad + \sum_{j=pq-d+1}^{pq} A_h^{pq-j} B_h \Gamma u(nT + (j-1)h - T,k) \\ &\quad + \sum_{j=pq-d+1}^{pq} A_h^{pq-j} D_h w(nT + (j-1)h - T,k). \end{aligned} \tag{10}$$

Similarly, we can directly obtain

$$\begin{aligned} x(nT+T,k) &= A_h^{pq} x(nT,k) \\ &\quad + \sum_{j=0}^{q-1}\sum_{i=1}^{p} A_h^{pq-jp-i} B_h \Gamma u\left[nT + jT_1 + (i-1)h, k\right] \\ &\quad + \sum_{j=0}^{q-1}\sum_{i=1}^{p} A_h^{pq-jp-i} D_h w\left[nT + jT_1 + (i-1)h, k\right], \end{aligned} \tag{11}$$

$$\begin{aligned} x(nT+\mathrm{T}-dh,k) &= A_h^{pq-d} x(nT,k) \\ &\quad + \sum_{j=1}^{pq-d} A_h^{pq-d-j} B_h \Gamma u\left(nT + (j-1)h, k\right) \\ &\quad + \sum_{j=1}^{pq-d} A_h^{pq-d-j} D_h w\left(nT + (j-1)h, k\right); \end{aligned} \tag{12}$$

according to (8), (11) can be simplified as

$$\begin{aligned} x(nT+T,k) &= A_h^{pq} x(nT,k) + \sum_{j=0}^{q-1}\sum_{i=1}^{p} A_h^{pq-jp-i} B_h \Gamma u\left(nT + jT_1, k\right) \\ &\quad + \sum_{j=0}^{q-1}\sum_{i=1}^{p} A_h^{pq-jp-i} D_h w\left[nT + jT_1 + (i-1)h, k\right]. \end{aligned} \tag{13}$$

Substituting (10) into (12) and defining $m := pd - d$, where we assume $pq > d$, we have

$$\begin{aligned} x(nT+T-dh,k) &= A_h^{pq} x(nT-dh,k) \\ &\quad + \sum_{j=m+1}^{pq} A_h^{pq+m-j} B_h \Gamma u\left(nT + (j-1)h - T, k\right) \\ &\quad + \sum_{j=1}^{m} A_h^{m-j} B_h \Gamma u\left(nT + (j-1)h, k\right) \\ &\quad + \sum_{j=1}^{m} A_h^{m-j} D_h w\left(nT + (j-1)h, k\right) \\ &\quad + \sum_{j=m+1}^{pq} A_h^{pq+m-j} D_h w\left(nT + (j-1)h - T, k\right). \end{aligned} \tag{14}$$

Remark 1. The assumption condition $pq > d$ can usually be satisfied for some dual-rate sampling processes; this means the time delay exists in the sampling frame period. Furthermore, if $pq \gg d$, then more information of the time delay system can be obtained in a full frame period when the controller is designed for the sampling process in Figure 1.

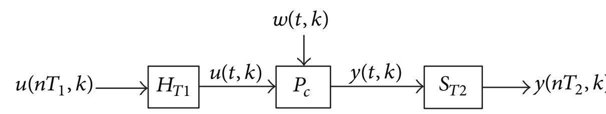

Figure 1: The general dual-rate sampling system.

In terms of lifting technology, defining the state expanding vector with $2n$ dimensions,

$$X(nT,k) = \begin{bmatrix} x(nT-dh,k) \\ x(nT,k) \end{bmatrix}, \tag{15}$$

and the input and disturbance expanding vectors with $(pd + d)$ dimensions,

$$\begin{aligned} U_z(nT,k) &= \begin{bmatrix} u(nT-dh,k) \\ u(nT-dh+h,k) \\ \vdots \\ u(nT+(pq-1)h,k) \end{bmatrix}, \\ W_z(nT,k) &= \begin{bmatrix} w(nT-dh,k) \\ w(nT-dh+h,k) \\ \vdots \\ w(nT+(pq-1)h,k) \end{bmatrix}, \end{aligned} \tag{16}$$

we can directly convert the dual-rate sampling system model (9) with output delay into a lifting linear discrete system model without delay in a single slow sampling rate $T = pqh$,

$$\begin{aligned} X(nT+T,k) &= A_z X(nT,k) + B_z \Gamma_z U_z(nT,k) \\ &\quad + D_z W_z(nT,k), \\ y(nT,k) &= C_z X(nT,k), \end{aligned} \tag{17}$$

where

$$\begin{aligned} A_z &= \begin{bmatrix} A & 0_{[n\times n]} \\ \star & A \end{bmatrix}, \\ B_z &= \begin{bmatrix} B & 0_{[n\times d]} \\ \star & B \end{bmatrix}, \\ C_z &= \begin{bmatrix} C_h & 0_{[1\times n]} \end{bmatrix}, \\ D_z &= \begin{bmatrix} D & 0_{[n\times d]} \\ \star & D \end{bmatrix}, \\ A &= A_h^{pq}, \\ \Gamma_z &= \operatorname{diag}\{\Gamma, \Gamma, \ldots, \Gamma\}, \\ B &= \begin{bmatrix} A_h^{pq-1} B_h & A_h^{pq-2} B_h & \cdots & A_h B_h & B_h \end{bmatrix}, \\ D &= \begin{bmatrix} A_h^{pq-1} D_h & A_h^{pq-2} D_h & \cdots & A_h D_h & D_h \end{bmatrix}. \end{aligned} \tag{18}$$

We can obviously find that although (17) is a slow sampling rate system with $T = pqh$, every real control input variable of expanding vector $U_z(nT,k)$ in (16) is also updated with a relatively fast sampling period h. Particularly, if we force the input variables to be updated just in slow sampling period T, that is, $u(nT-dh,k) = u(nT-(d-1)h,k) = \cdots = u(nT-h,k)$, $u(nT,k) = u(nT+h,k) = \cdots = u(nT+T-h,k)$, then (17) can be described as

$$U_s(nT,k) = \begin{bmatrix} u(nT-T,k) \\ u(nT,k) \end{bmatrix}; \tag{19}$$

thus we can get the discrete state-space model of the dual-rate sampling process (1) with one sampling period T; it is just a special form of (17):

$$\begin{aligned} X(nT+T,k) &= A_s X(nT,k) + B_s \Gamma_s U_s(nT,k) \\ &\quad + D_s W_z(nT,k), \\ y(nT,k) &= C_s X(nT,k), \end{aligned} \tag{20}$$

where

$$\begin{aligned} A_s &= A_z, \\ C_s &= C_z, \\ D_s &= D_z, \\ \Gamma_s &= \operatorname{diag}\{\Gamma,\Gamma\}, \\ B_s &= \begin{bmatrix} A_h^{pq-1}B_h + A_h^{pq-d-1}B_h + \cdots + A_h^{pq-d}B_h & A_h^{pq-d-1}B_h + \cdots + B_h \\ 0 & A_h^{pq-1}B_h + A_h^{pq-d-1}B_h + \cdots + B_h \end{bmatrix}. \end{aligned} \tag{21}$$

3. ILC Law Design

For the discrete sampling system described by (17), design an ILC law that constructs the current trial input that is equal to the control input on the previous trial plus a corrective term, that is, a control law of the form

$$U_z(nT,k+1) = U_z(nT,k) + r(nT,k+1), \tag{22}$$

where $r(nT,k)$ is the correction term computed using previous trial data. Given the reference signal $y_r(nT)$, the error on trial k is

$$e(nT,k) = y_r(nT) - y(nT,k). \tag{23}$$

To formulate the ILC design problem in the repetitive process setting, for analysis purpose only, we define the vectors

$$\begin{aligned} \eta(nT+T,k+1) &= X(nT,k+1) - X(nT,k), \\ \omega(nT+T,k+1) &= W_z(nT,k+1) - W_z(nT,k), \end{aligned} \tag{24}$$

$$\begin{aligned} \mu(nT+T,k+1) &= y(nT,k+1) - y(nT,k) \\ &= C_z \eta(nT+T,k+1). \end{aligned} \tag{25}$$

Without loss of generality, it is assumed that $y_r(0) = y(0,k) = C_z X(0,k)$ and, due to the initial conditions assumed for (17), $\mu(0,k) = 0$.

Since we can just obtain measurable input and output signal for dual-rate sampling process, suppose that the modification term in the output information based ILC law (22) takes the form

$$\begin{aligned} r(nT,k+1) &= K_1 \mu(nT+T,k+1) \\ &\quad + K_2 e(nT+T,k), \end{aligned} \tag{26}$$

where K_1 and K_2 are the control law matrices to be determined. Moreover, by (22)–(26) the controlled ILC dynamics can be written in the form of discrete repetitive process as

$$\begin{aligned} \eta(nT+T,k+1) &= \mathscr{A}\eta(nT,k+1) + \mathscr{B}_0 e(nT,k) \\ &\quad + \mathscr{B}_{11}\omega(nT,k+1), \\ e(nT,k+1) &= \mathscr{C}\eta(nT,k+1) + \mathscr{D}_0 e(nT,k) \\ &\quad + \mathscr{B}_{12}\omega(nT,k+1), \end{aligned} \tag{27}$$

where

$$\begin{aligned} \mathscr{A} &= A_z + B_z\Gamma_z K_1 C_z, \\ \mathscr{B}_0 &= B_z \Gamma_z K_2, \\ \mathscr{B}_{11} &= D_z, \\ \mathscr{C} &= -C_z A_z + C_z B_z \Gamma_z K_1 C_z, \\ \mathscr{D}_0 &= I - C_z B_z \Gamma_z K_2, \\ \mathscr{B}_{12} &= -C_z D_z. \end{aligned} \tag{28}$$

The state-space model (27) represents a linear discrete repetitive process with pass output $e(nT,k)$ and state vectors $\eta(nT,k)$, respectively, once the initial conditions are specified, that is, the pass state initial vector $\eta(0,k)$, $k \geq 1$, and the initial pass profile $e(nT,0)$.

Remark 2. It is important to stress that, with the ILC law (22) applied, the resulting controlled dynamics (27) are modeled by a linear repetitive process state-space model; the previous trial (pass) error $e(nT,k)$ affects the current trial (pass) error

$e(nT, k+1)$. Repetitive process is a particular class of 2D systems where a series of sweeps are made through a set of dynamics defined over a finite duration. Once each sweep is completed, the dynamics are reset and the next sweep starts. On any sweep, the output on the previous sweep explicitly contributes to the current sweep output and hence the link to ILC dynamics [24].

Next the representation of discrete repetitive processes and the associated stability theory are given as background.

4. Repetitive Process Theory

The state-space model of a linear discrete repetitive process over the finite pass length α is

$$\begin{aligned} x(t+1,k+1) &= \mathscr{A}x(t,k+1) + \mathscr{B}u(t,k+1) \\ &\quad + \mathscr{B}_0 y(t,k) + \mathscr{B}_{11} w(t,k+1), \\ y(t,k+1) &= \mathscr{C}x(t,k+1) + \mathscr{D}u(t,k+1) \\ &\quad + \mathscr{D}_0 y(t,k) + \mathscr{B}_{12} w(t,k+1), \end{aligned} \tag{29}$$

where, on pass k, $x(t,k)$ is the state vector, $y(t,k)$ is the output vector, $u(t,k)$ is the control input vector, and $w(t,k+1)$ is the disturbance input vector. If

$$\|\omega(t,k+1)\|_{\ell_2} = \sqrt{\sum_{t=0}^{N_1}\sum_{k=0}^{N_2}\|\omega(t,k+1)\|^2} < \infty \tag{30}$$

for any integers $N_1, N_2 > 0$, then $w(t,k+1)$ is in ℓ_2 space, denoted by $w(t,k+1) \in \ell_2$. To complete the process description, it is necessary to specify the boundary conditions, that is, the pass state initial vector sequence $x(0,k)$, $k \geq 1$, and the initial pass profile $y(t,0)$.

Define the shift operators z_1, z_2 along the pass (t) and pass-to-pass (k) directions acting, for example, on $x(t+1,k)$ and $y(t,k+1)$, respectively, as

$$\begin{aligned} x(t,k) &:= z_1 x(t+1,k), \\ y(t,k) &:= z_2 x(t,k+1); \end{aligned} \tag{31}$$

then the 2D characteristic polynomial for processes described by (29) is defined as

$$\mathfrak{I}(z_1,z_2) = \det\left(\begin{bmatrix} I - z_1\mathscr{A} & -z_1\mathscr{B}_0 \\ -z_2\mathscr{C} & I - z_2\mathscr{D}_0 \end{bmatrix}\right); \tag{32}$$

the stability along the pass holds if and only if

$$\begin{aligned} \mathfrak{I}(z_1,z_2) &= \det\left(I - z_1\mathscr{A}_1 - z_2\mathscr{A}_2\right) \neq 0, \\ &\qquad \text{if } |z_1| \leq 1,\ |z_2| \leq 1, \end{aligned} \tag{33}$$

where

$$\mathscr{A}_1 = \begin{bmatrix} \mathscr{A} & \mathscr{B}_0 \\ 0 & 0 \end{bmatrix}, \qquad \mathscr{A}_2 = \begin{bmatrix} 0 & 0 \\ \mathscr{C} & \mathscr{D}_0 \end{bmatrix}. \tag{34}$$

This reversely promotes the development of LMI based stability condition along the pass which are sufficient but not necessary.

Lemma 3 (see [24]). *A linear discrete repetitive process described by (29) is stable along the pass if there exists a block-diagonal matrix $P \succ 0$ such that the following LMI holds:*

$$\Phi^T P \Phi - P \prec 0, \tag{35}$$

where

$$\Phi = \begin{bmatrix} \mathscr{A} & \mathscr{B}_0 \\ \mathscr{C} & \mathscr{D}_0 \end{bmatrix} \tag{36}$$

is the so-called augmented plant matrix.

Definition 4. A linear discrete repetitive process described by (29) is said to have H_∞ robust disturbance attenuation γ if it is stable along the pass and

$$\sup_{0\neq w\in l_2} \frac{\|y(t,k+1)\|_{\ell_2}}{\|w(t,k+1)\|_{\ell_2}} < \gamma. \tag{37}$$

Now consider the 2D transfer function matrix coupling the disturbance and current pass profile vectors which is given by

$$G_{yw}(z_1,z_2) = \begin{bmatrix} 0 & I \end{bmatrix} \begin{bmatrix} I - z_1\mathscr{A} & -z_1\mathscr{B}_0 \\ -z_2\mathscr{C} & I - z_2\mathscr{D}_0 \end{bmatrix}^{-1} \begin{bmatrix} \mathscr{B}_{11} \\ \mathscr{B}_{12} \end{bmatrix} \tag{38}$$

and then the 2D Parseval theorem, which states that (37) is equivalent to the requirement that

$$\left\|G_{yw}(z_1,z_2)\right\| = \sup_{w_1,w_2\in[0,2\pi]} \overline{\sigma}\left[G_{yw}\left(e^{jw_1}, e^{jw_2}\right)\right] < \gamma, \tag{39}$$

where $\overline{\sigma}(\cdot)$ denotes the maximum singular value [34].

5. Stability Analysis

The following lemmas are used in the proofs of the main results.

Lemma 5 (Schur complement formula [35]). *Given a symmetric matrix $\mathcal{S} = \left[\begin{smallmatrix} \mathcal{S}_{11} & \mathcal{S}_{12} \\ \mathcal{S}_{21} & \mathcal{S}_{22} \end{smallmatrix}\right]$, $\mathcal{S}_{11}$ and $\mathcal{S}_{22}$ are square matrices, and then the following inequalities are equivalent:*

(i) $\mathcal{S} \prec 0$.

(ii) $\mathcal{S}_{11} \prec 0$ *and* $\mathcal{S}_{22} - \mathcal{S}_{12}^T\mathcal{S}_{11}^{-1}\mathcal{S}_{12} \prec 0$.

(iii) $\mathcal{S}_{22} \prec 0$ *and* $\mathcal{S}_{11} - \mathcal{S}_{12}^T\mathcal{S}_{22}^{-1}\mathcal{S}_{12} \prec 0$.

Lemma 6 (see [36]). *Given matrices X, Y, $\Omega = \Omega^T$, and $\delta(t)$ of compatible dimensions, then*

$$\Omega + X\delta(t)Y + Y^T\delta^T(t)X^T \prec 0, \tag{40}$$

for all $\delta(t)$ satisfying $\delta^T(t)\delta(t) \preceq I$ if and only if there exists some $\varepsilon > 0$ such that

$$\Omega + \varepsilon XX^T + \varepsilon^{-1}Y^TY \prec 0. \tag{41}$$

Theorem 7. *Assume repetitive disturbance $w(t,k)$ exists in dual-rate sampling process P_c, that is, $\omega(nT,k+1) = 0$ in discrete repetitive process (27); for any $\varepsilon > 0$, output information based ILC scheme described as (27) under an actuator fault of the form (3)–(6) is stable along the trial, if there exist matrices $Q = \operatorname{diag}\{Q_1, Q_2\} \succ 0$, N, M, and L such that*

$$C_z Q_1 = M C_z, \tag{42}$$

$$\begin{bmatrix} -Q & \star & \star \\ R_1 & -Q & \star \\ R_2 & R_3 & -\varepsilon I \end{bmatrix} \prec 0 \tag{43}$$

hold, where $q_z = \operatorname{diag}\{q, q, \ldots, q\}$, $q_{0z} = \operatorname{diag}\{q_0, q_0, \ldots, q_0\}$, and

$$\begin{aligned} R_1 &= \begin{bmatrix} A_z Q_1 + B_z q_z N C_z & B_z q L \\ -C_z A_z Q_1 - C_z B_z q_z N C_z & Q_2 - C_z B_z q_z L \end{bmatrix}, \\ R_2 &= \begin{bmatrix} 0 & 0 \\ q_z N C_z & q_z L \end{bmatrix}, \\ R_3 &= \begin{bmatrix} \varepsilon q_0 B_z^T & -\varepsilon q_{0z} (B_z C_z)^T \\ 0 & 0 \end{bmatrix}; \end{aligned} \tag{44}$$

then the corresponding matrices in output information based control law (26) are given by

$$\begin{aligned} K_1 &= N M^{-1}, \\ K_2 &= L Q_2^{-1}. \end{aligned} \tag{45}$$

Proof. According to Lemma 3, we have $\Phi^T P \Phi - P \prec 0$, where $P = \operatorname{diag}\{P_1, P_2\} \succ 0$, and

$$\Phi = \begin{bmatrix} A_z + B_z \Gamma_z K_1 C_z & B_z \Gamma_z K_2 \\ -C_z A_z - C_z B_z \Gamma_z K_1 C_z & I - C_z B_z \Gamma_z K_2 \end{bmatrix}. \tag{46}$$

Applying Lemma 5 (Schur's complement formula) to $\Phi^T P \Phi - P \prec 0$ gives

$$\begin{bmatrix} -P_1 & \star & \star & \star \\ 0 & -P_2 & \star & \star \\ A_z + B_z \Gamma_z K_1 C_z & B_z \Gamma_z K_2 & -P_1^{-1} & \star \\ -C_z A_z - C_z B_z \Gamma_z K_1 C_z & I - C_z B_z \Gamma_z K_2 & 0 & -P_2^{-1} \end{bmatrix} \prec 0. \tag{47}$$

Introduce $Q_1 = P_1^{-1}$ and $Q_2 = P_2^{-1}$, and pre- and postmultiply (47) by matrix $\operatorname{diag}\{Q_1, Q_2, I, I\}$ to yield

$$\begin{bmatrix} -Q_1 & \star & \star & \star \\ 0 & -Q_2 & \star & \star \\ A_z + B_z \Gamma_z K_1 C_z Q_1 & B_z \Gamma_z K_2 Q_2 & -Q_1 & \star \\ -C_z A_z - C_z B_z \Gamma_z K_1 C_z Q_1 & I - C_z B_z \Gamma_z K_2 Q_2 & 0 & -Q_2 \end{bmatrix} \prec 0. \tag{48}$$

Due to $\Gamma_z = \operatorname{diag}\{(I+\Gamma_0)q, (I+\Gamma_0)q, \ldots, (I+\Gamma_0)q\} = (I+\Gamma_{0z})q_z$ and $\Gamma_{0z} = \operatorname{diag}\{\Gamma_0, \Gamma_0, \ldots, \Gamma_0\}$, we can rewrite (48) as

$$H + X \Gamma_{0z} Y + (X \Gamma_{0z} Y)^T \prec 0, \tag{49}$$

where

$$\begin{aligned} X &= \begin{bmatrix} 0 & 0 & B_z^T & -(C_z B_z)^T \end{bmatrix}^T, \\ Y &= \begin{bmatrix} q_z K_1 C_z Q_1 & q_z K_2 Q_2 & 0 & 0 \end{bmatrix}, \\ H &= \begin{bmatrix} -Q_1 & \star & \star & \star \\ 0 & -Q_2 & \star & \star \\ (A_z + B_z q_z K_1 C_z) Q_1 & B_z q_z K_2 Q_2 & -Q_1 & \star \\ -(C_z A_z + C_z B_z q_z K_1 C_z) Q_1 & Q_2 - C_z B_z q_z K_2 Q_2 & 0 & -Q_2 \end{bmatrix}; \end{aligned} \tag{50}$$

then by Lemma 6 and (6), inequality (49) is feasible if and only if

$$H + \begin{bmatrix} \varepsilon^{1/2} X q_{0z} & \varepsilon^{-1/2} \; Y^T \end{bmatrix} \begin{bmatrix} \varepsilon^{1/2} q_{0z} X^T \\ \varepsilon^{-1/2} Y \end{bmatrix} \prec 0 \tag{51}$$

holds, where $q_{0z} = \operatorname{diag}\{q_0, q_0, \ldots, q_0\}$; then application of Schur's complement formula to (51) gives

$$\begin{bmatrix} H & \star & \star \\ \varepsilon^{1/2} q_{0z} X^T & -I & \star \\ \varepsilon^{-1/2} Y & 0 & -I \end{bmatrix} \prec 0. \tag{52}$$

Pre- and postmultiplying the above inequality by $\operatorname{diag}\{I, I, I, I, \varepsilon^{1/2} I, \varepsilon^{1/2} I\}$ and applying condition (42) immediately give the LMI of (43). This completes proof of the theorem. □

Suppose nonrepetitive disturbance $w(t,k)$ exists in dual-rate sampling process P_c, that is, $\omega(nT,k+1) \neq 0$ in repetitive process (27); then the H_∞ robust disturbance attenuation performance (37) should be modified as

$$\sup_{0 \neq w \in l_2} \frac{\|e(nT,k+1)\|_{\ell_2}}{\|\omega(nT,k+1)\|_{\ell_2}} < \gamma; \tag{53}$$

consequently, we can have the following result for robust controller design.

Theorem 8. *Assume $\omega(nT,k+1) \neq 0$; for any $\varepsilon > 0$, output information based ILC scheme described as a discrete linear repetitive process of the form (27) under an actuator fault of the form (3)–(6) is stable along the trial and has H_∞ disturbance attenuation $\gamma > 0$; hence if there exist matrices $Q = \operatorname{diag}\{Q_1, Q_2\} \succ 0$, N, M, and L such that*

$$\begin{bmatrix} -Q & \star & \star & \star & \star \\ 0 & -\gamma I & \star & \star & \star \\ R_1 & F & -Q & \star & \star \\ R_4 & 0 & 0 & -\gamma I & \star \\ R_2 & 0 & R_3 & 0 & -\varepsilon I \end{bmatrix} \prec 0 \tag{54}$$

holds, where R_1, R_2, R_3 are given in (44), $R_4 = [0 \;\; Q_2]$, $F = \begin{bmatrix} D_z^T & -D_z^T C_z^T \end{bmatrix}^T$, and the robust control law matrices K_1 and K_2 are given by (45).

Proof. Suppose there exists H_∞ robust disturbance attenuation γ if the associated Hamiltonian function

$$\begin{aligned} J(nT,k) = {} & \Delta V(nT,k) + \gamma^{-1} \|e(nT,k+1)\|^2 \\ & - \gamma \|\omega(nT,k+1)\|^2 < 0 \end{aligned} \tag{55}$$

holds, where $\Delta V(nT,k)$ is the associated increment of Lyapunov function for repetitive process (27):

$$\begin{aligned} V(nT,k) = {} & \eta^T(nT,k+1) P_1 \eta(nT,k+1) \\ & + e^T(nT,k) P_2 e(nT,k), \end{aligned} \tag{56}$$

where $P_1 \succ 0$, $P_2 \succ 0$, and

$$\begin{aligned} \Delta V(nT,k) = {} & \eta^T(nT+T,k+1) P_1 \eta(nT+T,k+1) \\ & + e^T(nT,k+1) P_2 e(nT,k+1) \\ & - \eta^T(nT,k+1) P_1 \eta(nT,k+1) \\ & - e^T(nT,k) P_2 e(nT,k). \end{aligned} \tag{57}$$

It is clear that (55) requires $\Delta V(nT,k) < 0$ and hence the result of Lemma 3 holds. Using (27), it is easily shown that

$$J(nT,k) = \begin{bmatrix} \eta(nT,k+1) \\ e(nT,k) \\ \omega(nT,k+1) \end{bmatrix}^T \Psi \begin{bmatrix} \eta(nT,k+1) \\ e(nT,k) \\ \omega(nT,k+1) \end{bmatrix} < 0, \tag{58}$$

where

$$\begin{aligned} \Psi = {} & \begin{bmatrix} \mathscr{A}^T P_1 \mathscr{A} + \mathscr{C}^T P_2 \mathscr{C} - P_1 & \mathscr{A}^T P_1 \mathscr{B}_0 + \mathscr{C}^T P_2 \mathscr{D}_0 & \mathscr{A}^T P_1 \mathscr{B}_{11} + \mathscr{C}^T P_2 \mathscr{B}_{12} \\ \star & \mathscr{B}_0^T P_1 B_0 + \mathscr{D}_0^T P_2 \mathscr{D}_0 - P_2 - \gamma^{-1} I & \mathscr{B}_0^T P_1 \mathscr{B}_{11} + \mathscr{D}_0^T P_2 \mathscr{B}_{12} \\ \star & \star & \mathscr{B}_{11}^T P_1 \mathscr{B}_{11} + \mathscr{B}_{12}^T P_2 \mathscr{B}_{12} - \gamma I \end{bmatrix} = \begin{bmatrix} \Phi^T \\ F^T \end{bmatrix} P \begin{bmatrix} \Phi & F \end{bmatrix} \\ & - \begin{bmatrix} P - \gamma^{-1} G^T G & 0 \\ 0 & \gamma I \end{bmatrix} \prec 0, \end{aligned} \tag{59}$$

and $G = [0 \;\; I]$ and $P = \operatorname{diag}\{P_1, P_2\}$. Applying the Schur complement formula to (59) and defining $Q = P^{-1} = \operatorname{diag}\{Q_1, Q_2\}$ give

$$\begin{bmatrix} -P & \star & \star & \star \\ 0 & -\gamma I & \star & \star \\ \Phi & F & -Q & \star \\ G & 0 & 0 & -\gamma I \end{bmatrix} \prec 0. \tag{60}$$

Moreover, pre- and postmultiplying (60) by $\operatorname{diag}\{Q, I, I, I\}$ and its transpose, respectively, we have

$$\begin{bmatrix} -Q & \star & \star & \star \\ 0 & -\gamma I & \star & \star \\ \Phi Q & F & -Q & \star \\ GQ & 0 & 0 & -\gamma I \end{bmatrix} \prec 0; \tag{61}$$

therefore, (61) also can be modified as

$$H' + X' \Gamma_{0z} Y' + \left(X' \Gamma_{0z} Y' \right)^T \prec 0, \tag{62}$$

where

$$\begin{aligned} X' &= \begin{bmatrix} 0 & 0 & 0 & B_z^T & -(C_z B_z)^T & 0 \end{bmatrix}^T, \\ Y' &= \begin{bmatrix} q_z K_1 C_z Q_1 & q_z K_2 Q_2 & 0 & 0 & 0 & 0 \end{bmatrix}, \end{aligned}$$

$$H' = \begin{bmatrix} -Q_1 & \star & \star & \star & \star & \star \\ 0 & -Q_2 & \star & \star & \star & \star \\ 0 & 0 & -\gamma I & \star & \star & \star \\ (A_z + B_z q_z K_1 C_z) Q_1 & B_z q_z K_2 Q_2 & D_z & -Q_1 & \star & \star \\ -(C_z A_z - C_z B_z q_z K_1 C_z) Q_1 & Q_2 - C_z B_z q_z K_2 Q_2 & -C_z D_z & 0 & -Q_2 & \star \\ 0 & Q_2 & 0 & 0 & 0 & -\gamma I \end{bmatrix}. \tag{63}$$

Similar to the proof of Theorem 7, another application of Lemmas 6 and 5 immediately gives (54).

The following analysis is to prove the H_∞ robust disturbance attenuation γ. For any positive integers N_1, N_2, when all the initial conditions $\eta(0,k)$ and $e(nT,0)$ in (57) are assumed to be zero, we have

$$\begin{aligned} &\sum_{n=0}^{N_1} \sum_{k=0}^{N_2} \Delta V(nT,k) \\ &\quad = \sum_{k=0}^{N_2} \eta((N_1+1)T, k+1)^T P_1 \eta((N_1+1)T, k+1) \\ &\qquad + \sum_{n=0}^{N_1} e(nT, N_2+1)^T P_2 e(nT, N_2+1) \ge 0. \end{aligned} \tag{64}$$

Using (55) and (64) yields

$$\begin{aligned} &\sum_{n=0}^{N_1} \sum_{k=0}^{N_2} \left(\gamma^{-1} \|e(nT,k+1)\|_{\ell_2}^2 - \gamma \|\omega(nT,k+1)\|_{\ell_2}^2\right) \\ &\quad \le \sum_{n=0}^{N_1} \sum_{k=0}^{N_2} \left(\Delta V(nT,k) + \gamma^{-1} \|e(nT,k+1)\|_{\ell_2}^2 \right. \\ &\qquad \left. - \gamma \|\omega(nT,k+1)\|_{\ell_2}^2\right) = \sum_{n=0}^{N_1} \sum_{k=0}^{N_2} J(nT,k) < 0; \end{aligned} \tag{65}$$

then (53) is satisfied; this means the ILC control process (27) has robust disturbance attenuation γ and the proof is complete. □

It should be emphasized that condition (42) is not an inequality form; it cannot be directly solved by LMI tools. Therefore, one can first determine Q_1, Q_2, N, and L by solving the LMI (43) or (54) and then get

$$M = C_z Q_1 C_z^+, \tag{66}$$

where C_z^+ is the right inverse of matrix C_z. However, in some cases, it is impossible to obtain the matrix M by using the above formulation. Therefore, condition (42) in Theorems 7 and 8 can be converted into the following inequality [37]:

$$(MC_z - C_z Q_1)^T (MC_z - C_z Q_1) \prec \zeta I, \tag{67}$$

where ζ is a sufficiently small positive scalar. Observe that if the value of the scalar ζ is sufficiently small, condition (42) is approximately satisfied. Thus one obtains the LMI condition using the Schur complement formula:

$$\begin{aligned} &\text{Minimize} \quad \zeta \\ &\text{subject to} \quad \begin{bmatrix} \zeta I & C_z Q_1 - MC_z \\ \star & \zeta I \end{bmatrix} \succ 0. \end{aligned} \tag{68}$$

6. Case Study

To illustrate the validity of the proposed design method, a system of two noninteracting flow tanks in series including pipelines and valves is considered for process control [38]. The material balance equations that govern the system in the disturbance-free and fault-free case shown in Figure 2 are

$$\begin{aligned} A_{c1} \frac{dh_1}{dt} &= F_i - c_1 h_1, \\ A_{c2} \frac{dh_2}{dt} &= c_1 h_1 - c_2 h_2, \end{aligned} \tag{69}$$

where A_{c1} and A_{c2} are the cross-sectional areas of tanks 1 and 2, unmeasurable states h_1 and h_2 are the liquid levels for tanks 1 and 2, c_1 and c_2 are constants which depend on the valves, and input F_i is the measured inlet flow rate. Meantime, amplifier element is used when the measured output signal outlet flow rate F_{o2} is very small and nominally equal to $5c_2h_2$. Thus (69) can be written in state-space form

$$\begin{aligned} \dot{x}(t,k) &= A_c x(t,k) + B_c u(t,k) \\ y(t,k) &= C_c x(t,k), \end{aligned} \tag{70}$$

where

$$A_c = \begin{bmatrix} \frac{-c_1}{A_{c_1}} & 0 \\ \frac{c_1}{A_{c_2}} & \frac{-c_2}{A_{c_2}} \end{bmatrix},$$

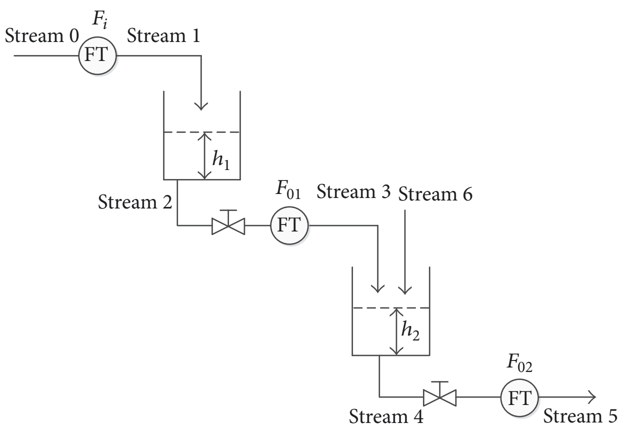

Figure 2: Simple structure diagram of two flow tanks in series.

$$B_c = \begin{bmatrix} \frac{1}{A_{c_1}} \\ 0 \end{bmatrix},$$

$$C_c = \begin{bmatrix} 0 & 5c_2 \end{bmatrix},$$

$$u(t,k) = F_i,$$

$$y(t,k) = F_{o2},$$

$$x^T(t,k) = \begin{bmatrix} h_1 & h_2 \end{bmatrix}. \tag{71}$$

Due to the differences of distance between the control points of tanks and flow rates to the sensors at the bottom of each tank, output time delay commonly appears in the system, which gives rise to instability and poor performance. Consider the case where the unknown external bounded disturbance stream (Stream 6 in Figure 2) is introduced into tank 2 for $t > 0$. The state-space form (71) becomes

$$\begin{aligned} \dot{x}(t,k) &= A_c x(t,k) + B_c u(t,k) + D_c w(t,k), \\ y(t,k) &= C_c x(t-\tau), \end{aligned} \tag{72}$$

where $w(t,k)$ represents the unknown external bounded disturbance stream and $\tau > 0$ is the fixed delay. In the following simulations, the model parameters used are $A_{c_1} = A_{c_2} = 0.8$, $c_1 = 0.3$, $c_2 = 0.2$, $\tau = 1$, $D_c = \begin{bmatrix} 0 & 0.1 \end{bmatrix}^T$, the input updating time $T_1 = h$ and the output sampling period $T_2 = 5h$, and then frame period $T = 5h$. Applying the Euler concretization method with a sampling period $h = 1s$ to (72) results in the following discrete system model of the form (9), where

$$A_h = \begin{bmatrix} 0.6873 & 0 \\ 0.2745 & 0.7788 \end{bmatrix},$$

$$B_h = \begin{bmatrix} 1.0424 \\ 0.1910 \end{bmatrix},$$

$$C_h = \begin{bmatrix} 0 & 1 \end{bmatrix},$$

$$D_h = \begin{bmatrix} 0 & 0.0834 \end{bmatrix}^T,$$

$$d = 1. \tag{73}$$

Partial degradation and wear from repeated control operation can lead to faults arising during the trials and it is assumed that an actuator fault occurs in the operation valve. As a numerical example, it is assumed that $0.6 \le \underline{\Gamma} \le \Gamma \le \overline{\Gamma} = 1$; hence $q = 0.8$ and $q_0 = 0.25$. Suppose no actuator faults occur before $k = 15$ trials have elapsed. Applying the lifting technology, this dual-rate sampling tank model can be converted into a lifting linear discrete model of the form (17), where

$$A_z = \begin{bmatrix} 0.1534 & 0 & 0 & 0 \\ 0.3994 & 0.2865 & 0 & 0 \\ 0 & 0 & 0.1534 & 0 \\ 0 & 0 & 0.3994 & 0.2865 \end{bmatrix},$$

$$B_z = \begin{bmatrix} 0.2326 & 0.3384 & 0.4924 & 0.7164 & 1.0424 & 0 \\ 0.5229 & 0.5521 & 0.5354 & 0.4349 & 0.191 & 0 \\ 0 & 0.2326 & 0.3384 & 0.4924 & 0.716 & 1.0424 \\ 0 & 0.5229 & 0.5521 & 0.5354 & 0.4349 & 0.191 \end{bmatrix}, \tag{74}$$

$$C_z = \begin{bmatrix} 0 & 1 & 0 & 0 \end{bmatrix},$$

$$D_z = \begin{bmatrix} 0 & 0 & 0 & 0 & 0 & 0 \\ 0.0186 & 0.0271 & 0.0394 & 0.0573 & 0.0834 & 0 \\ 0 & 0 & 0 & 0 & 0 & 0 \\ 0 & 0.0186 & 0.0271 & 0.0394 & 0.0573 & 0.0834 \end{bmatrix}.$$

If we also force the input variable F_i to be just updated in slow sampling period T, then $u(nT-h,k) = u(nT-T,k)$ and $u(nT,k) = u(nT+h,k) = u(nT+2h,k) = u(nT+3h,k) = u(nT+4h,k)$; hence the dual-rate sampling tank model can be of the form (19), where $A_s = A_z$, $C_s = C_z$, $D_s = D_z$, $B_s = \begin{bmatrix} A_h^4 B_h & A_h^3 B_h + A_h^2 B_h + A_h B_h + B_h \\ 0 & A_h^4 B_h + A_h^3 B_h + A_h^2 B_h + A_h B_h + B_h \end{bmatrix}$.

The initial state vector on each trial is assumed to be zero, $\forall k \geq 0$, and the reference trajectory is

$$y_r(nT) = \begin{cases} 0.001nT, & 0 \leq n < 100 \\ 0.5, & 100 \leq n < 200 \\ 0.0003nT + 0.2, & 200 \leq n < 300 \\ 0.65, & 300 \leq n \leq 400. \end{cases} \quad (75)$$

Introduce the root mean square (RMS) to evaluate tracking performance from trial to trial:

$$H(k) = \sqrt{\frac{1}{400}\sum_{n=1}^{400} e^2(nT, k)}, \quad (76)$$

where the smaller the value of $H(k)$, the better the tracking performance along the kth trial. Next two possible scenarios are considered.

Scenario 1 (repetitive disturbance with a constant fault). It is assumed that $w(nh, k) = 0.1\sin(0.2n)$ in this scenario; hence $\omega(nT, k+1) = 0$. Consider the case when the operating valve is always partially blocked in tank system (9). This constant partial fault causes the actuator to drop to 80% of its normal value; hence $\Gamma = 0.8$. For single-rate sampling system model with matrices $\{A_s, B_s, C_s\}$, using LMI toolbox to solve inequality (68) in Theorem 7 gives the corresponding matrices in (45) as

$$K_1 = [-0.4120 \quad -0.2312]^T, \\ K_2 = [0.2001 \quad 0.1058]^T \quad (77)$$

and achieves minimum $\zeta = 0.6148$. Furthermore, we can also obtain the dual-rate sampling controller matrices from matrices $\{A_z, B_z, C_z\}$:

$$K_1 = [-0.1457 \quad -0.1167 \quad -0.1017 \quad -0.0606 \quad 0.0241 \quad 0.0256]^T, \quad (78)$$
$$K_2 = [0.2821 \quad 0.2054 \quad 0.1716 \quad 0.0861 \quad -0.0846 \quad -0.0476]^T.$$

$\zeta = 0.0126$. Substituting (77) and (78) into (26) gets single-rate sampling and dual-rate sampling fault-tolerant ILC law (22), respectively. Based on (16), we can find that single-rate sampling controller is just updated in sampling time nT, but dual-rate sampling controller is updated in every sampling time nT, $nT+h$, $nT+2h$, $nT+3h$, and $nT+4h$; the total sample number of dual-rate sampling controllers is five times that of the single-rate sampling controllers. The simulation results of input, output, and tracking error are shown in Figures 3–9.

Before the constant fault occurs, the tracking error rapidly converges into a steady state from trail to trial. As soon as the fault occurs, the output responses deviate from the reference trajectory and the tracking performance deteriorates. However, the tracking performance can achieve an excellent level again after some trials and even restore it to the original level under the fault-tolerant controller. This result can be reflected clearly in Figure 3, where the values of RMS for different trials are presented. Obviously, compared with the single-rate sampling controller, the dual-rate sampling controller has the advantage of faster convergence which ensures the reliable stability of the tank system. The effectiveness of the proposed scheme is thus illustrated under both normal and fault scenario.

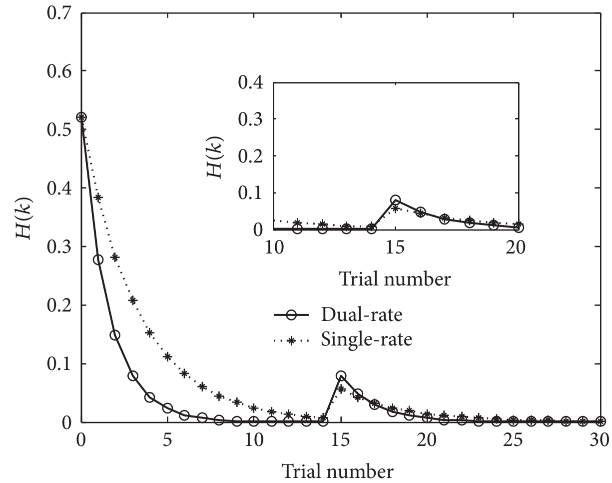

Dual-rate
Single-rate

FIGURE 3: The RMS performance for Scenario 1.

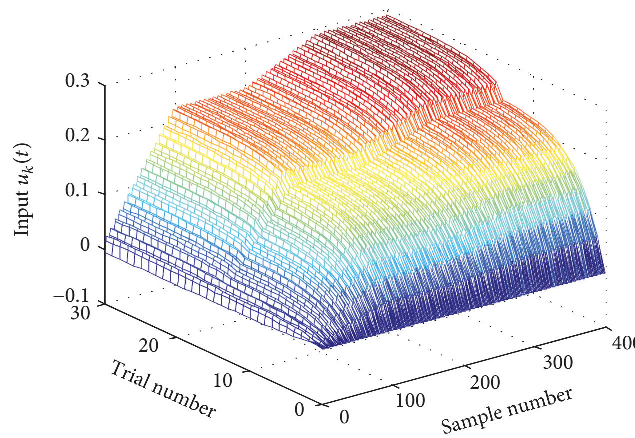

FIGURE 4: The single-rate input 3D curve for Scenario 1.

Scenario 2 (nonrepetitive disturbance with a time-varying fault). In this scenario, the operation valve is partly blocked by a time-varying fault in tank system (9), and the time-varying fault matrix $\Gamma = 0.8 + 0.2\sin(0.2n)$ is used here. In this case, nonrepetitive disturbance exists, and $w(nh, k) = 0.1\sin(0.01k)$ and $\omega(nT, k+1) \neq 0$. Solving the LMI of (68) in Theorem 8 also gives the single-rate and dual-rate ILC law matrices:

$$K_1 = [-0.6204 \quad -0.6236]^T, \\ K_2 = [0.3003 \quad 0.2233]^T. \quad (79)$$

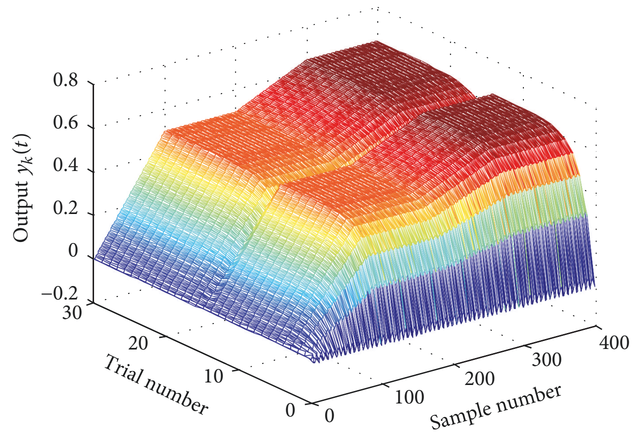

Figure 5: The single-rate output curve for Scenario 1.

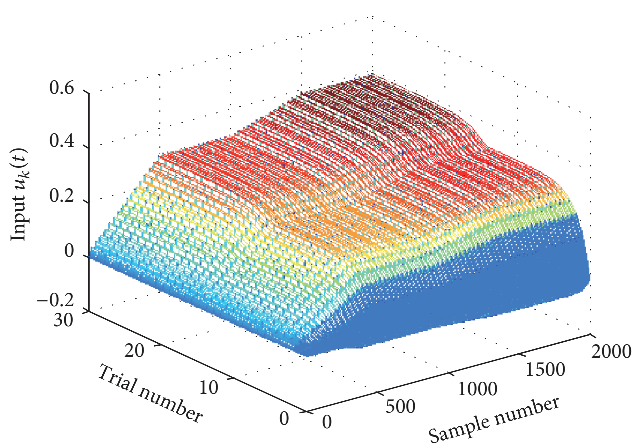

Figure 6: The dual-rate input 3D curve for Scenario 1.

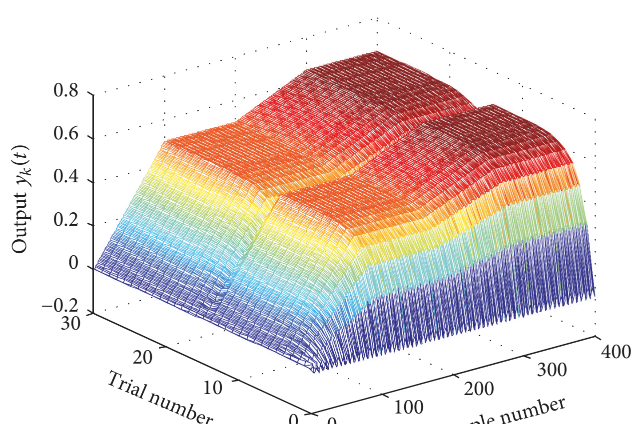

Figure 7: The dual-rate output curve for Scenario 1.

$\zeta = 0.6662$, and

$$K_1 = \begin{bmatrix} -0.4622 & -0.3833 & -0.3392 & -0.2128 & 0.0507 & 0.0811 \end{bmatrix}^T, \quad (80)$$

$$K_2 = \begin{bmatrix} 0.5141 & 0.3844 & 0.3072 & 0.1231 & -0.2366 & -0.0405 \end{bmatrix}^T.$$

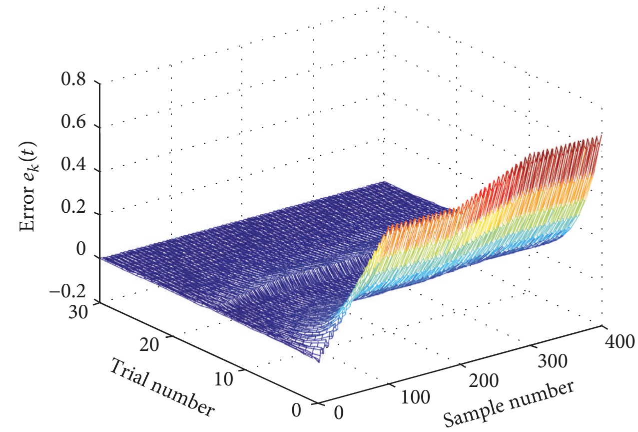

Figure 8: The single-rate tracking error 3D curve for Scenario 1.

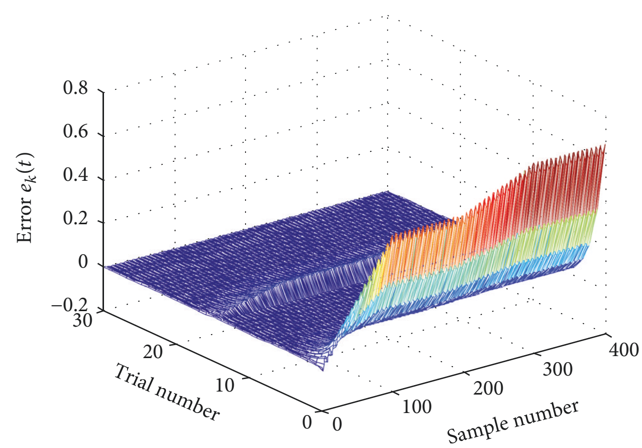

Figure 9: The dual-rate tracking error 3D curve for Scenario 1.

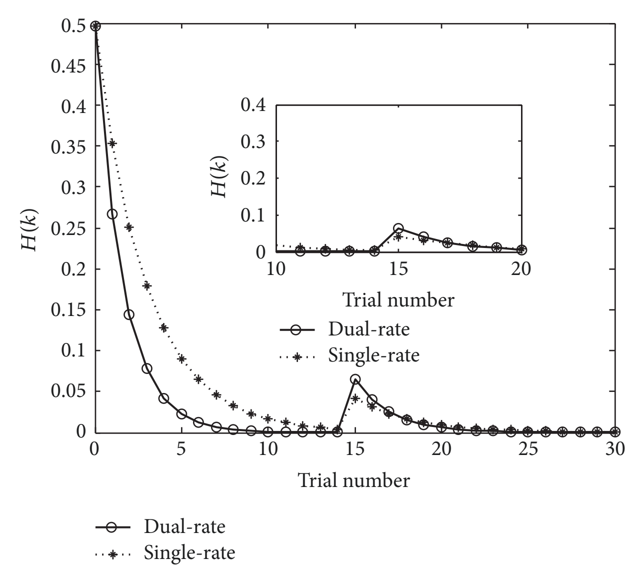

Figure 10: The RMS performance for Scenario 2.

$\zeta = 0.5205$, and the H_∞ disturbance attenuation is $\gamma = 1.3244$ and $\gamma = 1.1040$, respectively. The simulation results are shown in Figures 10–16. From these figures, the robustness

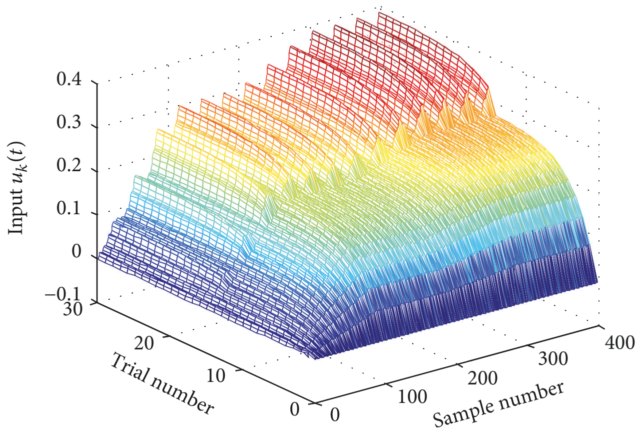

Figure 11: The single-rate input 3D curve for Scenario 2.

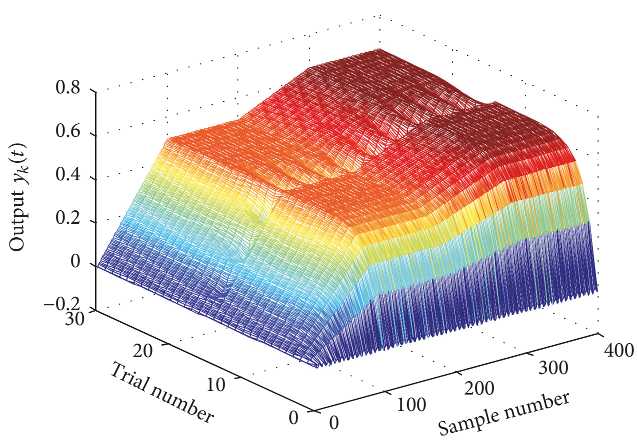

Figure 12: The single-rate output curve for Scenario 2.

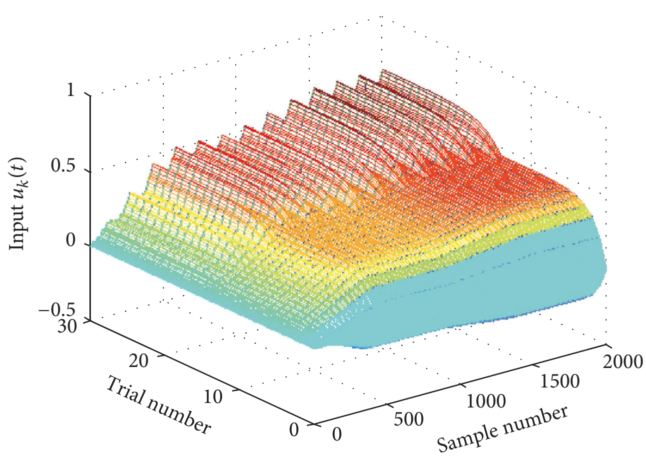

Figure 13: The dual-rate input 3D curve for Scenario 2.

and convergence of the designed control system along both sampling number and trial directions can be guaranteed even with a certain degree of nonrepetitive external disturbance.

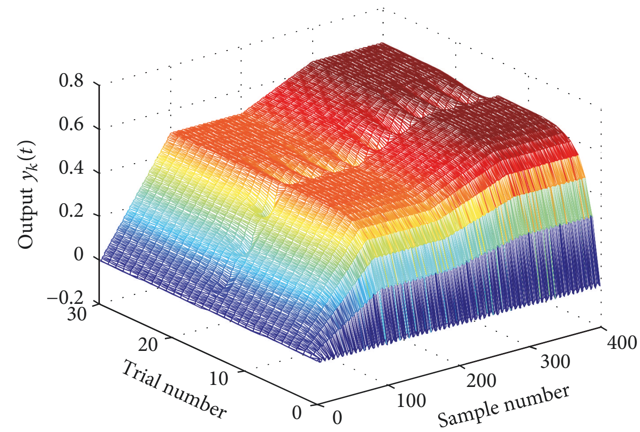

Figure 14: The dual-rate output curve for Scenario 2.

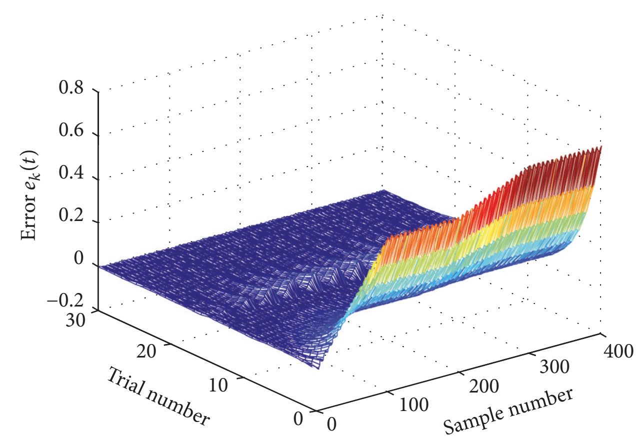

Figure 15: The single-rate tracking error 3D curve for Scenario 2.

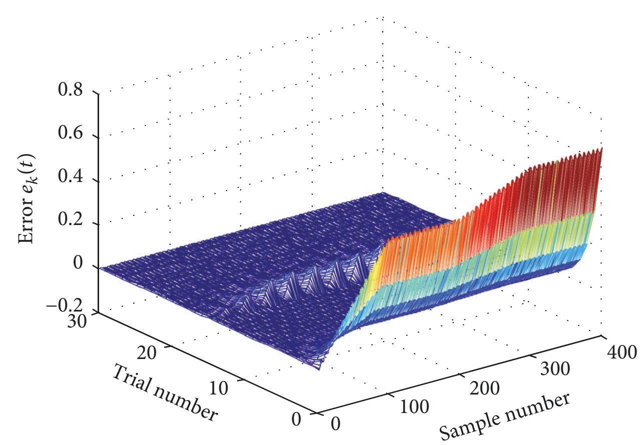

Figure 16: The dual-rate tracking error 3D curve for Scenario 2.

7. Conclusion and Future Works

This paper deals with the iterative learning fault-tolerant tracking control problem for a class of linear dual-rate sampling processes with actuator fault and output time delay. Firstly, the dual-rate sampling system is described in slow sampling rate model by lifting technology. Then we designed the output information based robust fault-tolerant ILC law based on the repetitive process theory. Sufficient conditions for the ILC law with stability and disturbance attenuation performance are given in terms of the corresponding linear matrix inequalities. Finally, the control simulation of the two noninteracting flow tanks in series verifies the effectiveness of this design method.

This proposed approach is not applicable for nonuniform sampling processes now; the uncertainty and time variation of the refresh time interval in nonuniform sampling processes make the system modeling very complicated by lifting technology. Moreover, the extension to multiple-input multiple-output systems may also cause computation burden issue when using expanding vector to design ILC law. But there are still many areas to which further research could profitably be directed. Possible further research directions include the optimization of H_∞ robust performance γ. Another area is to use the proposed control algorithm to deal with dual-rate sampling processes with external bounded disturbances in both the state and output sides. Extending the theory to simultaneously dispose state delay and input delay is also a possible topic for future work.

Conflicts of Interest

The authors declare that they have no conflicts of interest.

Acknowledgments

This work is supported by National Natural Science Foundation of China (61273070 and 61203092), 111 Project (B12018), the Fundamental Research Funds for the Central Universities (JUSRP51733B), the Enterprise-College-Institute Cooperative Project of Jiangsu Province (BY2015019-21), and the Priority Academic Program Development of Jiangsu Higher Education Institutions.

References

[1] J. Deng and B. Huang, "Identification of nonlinear parameter varying systems with missing output data," *AIChE Journal*, vol. 58, no. 11, pp. 3454–3467, 2012.

[2] S. Janardhanan and V. Kariwala, "Multirate-output-feedback-based LQ-optimal discrete-time sliding mode control," *Institute of Electrical and Electronics Engineers Transactions on Automatic Control*, vol. 53, no. 1, pp. 367–373, 2008.

[3] F. Ding and T. Chen, "Least squares based self-tuning control of dual-rate systems," *International Journal of Adaptive Control and Signal Processing*, vol. 18, no. 8, pp. 697–714, 2004.

[4] R. Scattolini, "Self-tuning control of systems with infrequent and delayed output sampling," *Institution of Electrical Engineers. Proceedings. D. Control Theory and Applications*, vol. 135, no. 4, pp. 213–221, 1988.

[5] W.-W. Ma, X.-C. Jia, and D.-W. Zhang, "Observer-based networked H∞ control for dualrate sampling systems," *Zidonghua Xuebao/Acta Automatica Sinica*, vol. 41, no. 10, pp. 1788–1797, 2015.

[6] L. Xie, H. Yang, and B. Huang, "FIR model identification of multirate processes with random delays using EM algorithm," *AIChE Journal*, vol. 59, no. 11, pp. 4124–4132, 2013.

[7] J. Chen, J. Li, and Y. Liu, "Gradient iterative algorithm for dual-rate nonlinear systems based on a novel particle filter," *Journal of The Franklin Institute*, vol. 354, no. 11, pp. 4425–4437, 2017.

[8] Y. Liu, F. Ding, and Y. Shi, "An efficient hierarchical identification method for general dual-rate sampled-data systems," *Automatica*, vol. 50, no. 3, pp. 962–970, 2014.

[9] Y. Guo and F. Liao, "Design of optimal output regulators for dual-rate linear discrete-time systems based on the lifting technique," *Mathematical Problems in Engineering*, vol. 2016, Article ID 2879724, 10 pages, 2016.

[10] D. Li, S. L. Shah, T. Chen, and K. Z. Qi, "Application of dual-rate modeling to CCR octane quality inferential control," *IEEE Transactions on Control Systems Technology*, vol. 11, no. 1, pp. 43–51, 2003.

[11] A. Üstüntürk, "Output feedback stabilization of nonlinear dual-rate sampled-data systems via an approximate discrete-time model," *Automatica*, vol. 48, no. 8, pp. 1796–1802, 2012.

[12] S. Arimoto, S. Kawamura, and F. Miyazaki, "Bettering operation of robots by learning," *Journal of Robotic Systems*, vol. 1, no. 2, pp. 123–140, 1984.

[13] H. Sun, Z. Hou, and D. Li, "Coordinated iterative learning control schemes for train trajectory tracking with overspeed protection," *IEEE Transactions on Automation Science and Engineering*, vol. 10, no. 2, pp. 323–333, 2013.

[14] D. Shen and Y. Wang, "Iterative learning control for networked stochastic systems with random packet losses," *International Journal of Control*, vol. 88, no. 5, pp. 959–968, 2015.

[15] C. T. Freeman, M. A. Alsubaie, Z. Cai, E. Rogers, and P. L. Lewin, "A common setting for the design of iterative learning and repetitive controllers with experimental verification," *International Journal of Adaptive Control and Signal Processing*, vol. 27, no. 3, pp. 230–249, 2013.

[16] J. Li and J. Li, "Iterative learning control approach for a kind of heterogeneous multi-agent systems with distributed initial state learning," *Applied Mathematics and Computation*, vol. 265, no. 8, pp. 1044–1057, 2015.

[17] Z. K. Nagy, "Model based robust control approach for batch crystallization product design," *Computers & Chemical Engineering*, vol. 33, no. 10, pp. 1685–1691, 2009.

[18] Y. Wang, D. Zhou, and F. Gao, "Iterative learning reliable control of batch processes with sensor faults," *Chemical Engineering Science*, vol. 63, no. 4, pp. 1039–1051, 2008.

[19] Y. Chen, B. Chu, and C. T. Freeman, "Point-to-point iterative learning control with optimal tracking time allocation," *IEEE Transactions on Control Systems Technology*, 2017.

[20] H. Ahn, Y. Q. Chen, and K. L. Moore, "Iterative learning control: brief survey and categorization," *IEEE Transactions on Systems, Man, and Cybernetics, Part C: Applications and Reviews*, vol. 37, no. 6, pp. 1099–1121, 2007.

[21] Y. Wang, F. Gao, and F. J. Doyle III, "Survey on iterative learning control, repetitive control, and run-to-run control," *Journal of Process Control*, vol. 19, no. 10, pp. 1589–1600, 2009.

[22] D. A. Bristow, M. Tharayil, and A. G. Alleyne, "A survey of iterative learning control: a learning-based method for high-performance tracking control," *IEEE Control Systems Magazine*, vol. 26, no. 3, pp. 96–114, 2006.

[23] E. Rogers, K. Galkowski, W. Paszke et al., "Multidimensional control systems: case studies in design and evaluation," *Multidimensional Systems and Signal Processing. An International Journal*, vol. 26, no. 4, pp. 895–939, 2015.

[24] E. Rogers, K. Galkowski, and D. H. Owens, "Control systems theory and applications for linear repetitive processes," *Lecture Notes in Control and Information Sciences*, vol. 349, pp. 1–476, 2007.

[25] H. D. Choi, C. K. Ahn, P. Shi, L. Wu, and M. T. Lim, "Dynamic output-feedback dissipative control for T-S fuzzy systems with time-varying input delay and output constraints," *IEEE Transactions on Fuzzy Systems*, vol. 25, no. 3, pp. 511–526, 2017.

[26] K. Gu, V. L. Kharitonov, and J. Chen, *Stability of Time Delay Systems*, Springer-Verlag, Berlin, Germany, 2003.

[27] L. Wang, S. Mo, D. Zhou, F. Gao, and X. Chen, "Delay-range-dependent robust 2D iterative learning control for batch processes with state delay and uncertainties," *Journal of Process Control*, vol. 23, no. 5, pp. 715–730, 2013.

[28] T. Liu and F. Gao, "Robust two-dimensional iterative learning control for batch processes with state delay and time-varying uncertainties," *Chemical Engineering Science*, vol. 65, no. 23, pp. 6134–6144, 2010.

[29] L. Wang, S. Mo, D. Zhou, F. Gao, and X. Chen, "Robust delay dependent iterative learning fault-tolerant control for batch processes with state delay and actuator failures," *Journal of Process Control*, vol. 22, no. 7, pp. 1273–1286, 2012.

[30] R. Sakthivel, B. Kaviarasan, and C. K. Ahn, "Observer and stochastic faulty actuator-based reliable consensus protocol for multiagent system," *IEEE Transactions on Systems Man Cybernetics Systems*, no. 99, pp. 1–11, 2017.

[31] J. Ding, B. Cichy, K. Galkowski, E. Rogers, and H.-Z. Yang, "Robust fault-tolerant iterative learning control for discrete systems via linear repetitive processes theory," *International Journal of Automation and Computing*, vol. 12, no. 3, pp. 254–265, 2015.

[32] H. Tao, W. Paszke, E. Rogers, H. Yang, and K. Gałkowski, "Iterative learning fault-tolerant control for differential time-delay batch processes in finite frequency domains," *Journal of Process Control*, vol. 56, pp. 112–128, 2017.

[33] L. Chen, L. Han, B. Huang, and F. Liu, "Parameter estimation for a dual-rate system with time delay," *ISA Transactions*, vol. 53, no. 5, pp. 1368–1376, 2014.

[34] W. Paszke, K. Galkowski, E. Rogers, and D. H. Owens, "H∞ and guaranteed cost control of discrete linear repetitive processes," *Linear Algebra and Its Applications*, vol. 412, no. 2-3, pp. 93–131, 2006.

[35] S. Boyd, L. El Ghaoui, E . Feron, and V. Balakrishnan, *Linear Matrix Inequalities in System and Control Theory*, SIAM, Philadelphia, Pa, USA, 1994.

[36] L. Xie, "Output feedback H∞ control of systems with parameter uncertainty," *International Journal of Control*, vol. 63, no. 4, pp. 741–750, 1996.

[37] Z. Gao, B. Jiang, P. Shi, J. Liu, and Y. Xu, "Passive fault-tolerant control design for near-space hypersonic vehicle dynamical system," *Circuits, Systems and Signal Processing*, vol. 31, no. 2, pp. 565–581, 2012.

[38] L. H. Chiang, E. L. Russell, and R. D. Braatz, *Fault Detection and Diagnosis in Industrial Systems*, Springer-Verlag, London, Britain, 2001.